doi:10.1093/brain/awl371 *Brain* (2007), **130**, 1194–1205

Pattern-specific loss of aquaporin-4 immunoreactivity distinguishes neuromyelitis optica from multiple sclerosis

Shanu F. Roemer,[1] Joseph E. Parisi,[2] Vanda A. Lennon,[1–3] Eduardo E. Benarroch,[1] Hans Lassmann,[4] Wolfgang Bruck,[5] Raul N. Mandler,[6] Brian G. Weinshenker,[1] Sean J. Pittock,[1,2] Dean M. Wingerchuk[7] and Claudia F. Lucchinetti[1]

Departments of [1]Neurology, [2]Laboratory Medicine and Pathology and [3]Immunology, Mayo Clinic College of Medicine, Rochester, MN, USA, [4]Center for the Clinical Trials Network, National Institutes of Health, Bethesda, MD , [5]Department of Neurology, Mayo Clinic College of Medicine, Scottsdale, AZ, USA, [6]Center for Brain Research, Medical University of Vienna, Vienna, Austria and [7]Department of Neuropathology, Institute for Multiple Sclerosis Research, Georg-August University, Gottingen, Germany

Correspondence to: Claudia F. Lucchinetti, MD, Neurology, Mayo Clinic, College of Medicine, 200 First St. SW, Rochester, MN 55905, USA
E-mail: lucchinetti.claudia@mayo.edu

Neuromyelitis optica (NMO) is an inflammatory demyelinating disease that typically affects optic nerves and spinal cord. Its pathogenic relationship to multiple sclerosis (MS) is uncertain. Unlike MS, NMO lesions are characterized by deposits of IgG and IgM co-localizing with products of complement activation in a vasculocentric pattern around thickened hyalinized blood vessels, suggesting a pathogenic role for humoral immunity targeting an antigen in the perivascular space. A recently identified specific serum autoantibody biomarker, NMO-IgG, targets aquaporin-4 (AQP4), the most abundant water channel protein in the CNS, which is highly concentrated in astrocytic foot processes. We analysed and compared patterns of AQP4 immunoreactivity in CNS tissues of nine patients with NMO, 13 with MS, nine with infarcts and five normal controls. In normal brain, optic nerve and spinal cord, the distribution of AQP4 expression resembles the vasculocentric pattern of immune complex deposition observed in NMO lesions. In contrast to MS lesions, which exhibit stage-dependent loss of AQP4, all NMO lesions demonstrate a striking loss of AQP4 regardless of the stage of demyelinating activity, extent of tissue necrosis, or site of CNS involvement. We identified a novel NMO lesion in the spinal cord and medullary tegmentum extending into the area postrema, characterized by AQP4 loss in foci that were inflammatory and oedematous, but neither demyelinated nor necrotic. Foci of AQP4 loss coincided with sites of intense vasculocentric immune complex deposition. These findings strongly support a role for a complement activating AQP4-specific autoantibody as the initiator of the NMO lesion, and further distinguish NMO from MS.

Keywords: neuromyelitis optica; aquaporin-4; multiple sclerosis; demyelination; astrocyte; blood–brain barrier

Abbreviations: AQP4 = aquaporin-4; HIVE = human immunodeficiency virus encephalitis; GFAP = glial fibrillary acidic protein; NMO = Neuromyelitis optica; PML = progressive multifocal leucoencephalopathy

Received August 25, 2006. Revised November 3, 2006. Accepted December 12, 2006. Advance Access publication February 5, 2007

Introduction

Neuromyelitis optica (NMO) is an idiopathic and usually relapsing inflammatory demyelinating disease of the CNS characterized by severe attacks of optic neuritis and myelitis. It can be distinguished from classical multiple sclerosis (MS) by clinical, neuroimaging, CSF and serological criteria (Wingerchuk *et al.*, 1999, 2006). In contrast to classical MS, which is thought to be mediated by effector T cells, increasing evidence supports a role for an autoantibody-mediated pathogenesis in NMO (Lucchinetti *et al.*, 2002). NMO is often associated with

other organ-specific or non-organ-specific autoimmune disorders, and a variety of serum autoantibodies (O'Riordan *et al.*, 1996; Wingerchuk *et al.*, 2006). In addition, plasmapheresis is therapeutically effective in NMO patients with severe steroid-unresponsive relapses (Keegan *et al.*, 2002). NMO lesions are characterized by extensive demyelination with partial necrosis in the spinal cord, involving both grey and white matter, and usually extending over multiple segments (Lucchinetti *et al.*, 2005). The lesions are associated with acute axonal injury, and inflammatory cell infiltrates containing eosinophils and granulocytes. Deposits of IgG and IgM co-localize with products of complement activation in a vasculocentric pattern around thickened hyalinized blood vessels, suggesting a pathogenic role for humoral immunity targeting an antigen in the perivascular space (Lucchinetti *et al.*, 2002). This hypothesis is strengthened by the recent identification of a specific serum autoantibody biomarker, NMO-IgG (Lennon *et al.*, 2004), which targets the most abundant water channel protein in the CNS aquaporin-4 (AQP4), (Lennon *et al.*, 2005).

The anatomical distribution and cellular sites of AQP4 expression in normal mammalian tissues, including brain and spinal cord, have been investigated extensively. AQP4 is a homotetrameric integral plasma membrane protein anchored in the astrocytic foot process membrane by the dystroglycan complex (Amiry-Moghaddam and Ottersen, 2003). Prior studies demonstrate intense AQP4 immunoreactivity in the plasma membrane of the astrocytic endfeet that abut capillaries and pia in the brain and spinal cord, particularly in the subpial and subependymal zones, as well as in the glial lamellae of the supraoptic nucleus in the hypothalamus (Jung *et al.*, 1994; Frigeri *et al.*, 1995; Nielsen *et al.*, 1997; Venero *et al.*, 1999; Amiry-Moghaddam and Ottersen, 2003).

The localization of AQP4 in the astrocytic foot processes surrounding endothelial cells is consistent with the role of astrocytes in the development, function and integrity of the interface between brain parenchyma and perivascular space, and between brain and cerebrospinal fluid, and serves to mediate water flux (Nicchia *et al.*, 2004). Experimental rodent models of ischaemia, trauma and hyponatraemia implicate AQP4 in the development of brain oedema regardless of cause (Manley *et al.*, 2000; Taniguchi *et al.*, 2000; Saadoun *et al.*, 2002; Vajda *et al.*, 2002; Warth *et al.*, 2005).

Enhanced AQP4 expression has been reported in a wide spectrum of human neuropathological conditions, including ischaemia, trauma, brain tumours, bacterial meningitis, progressive multifocal leucoencephalopathy (PML), human immunodeficiency virus encephalitis (HIVE), MS and Creutzfeldt–Jakob disease (Saadoun *et al.*, 2002; Aoki *et al.*, 2003, 2005; Misu *et al.*, 2006). A recent report (Aoki *et al.*, 2005), suggests that the distribution of intensely AQP4-positive astrocytes differs among disease states. In PML and HIVE, abundant AQP4-expressing astrocytes were noted at the boundary between grey and white matter apparently unrelated to inflammatory foci. The absence of a comparative analysis of AQP4 expression in normal control brain tissue in this study, however, may have led to erroneous attribution of AQP4 expression patterns to disease states. Additionally, rostral–caudal regional differences in AQP4 mRNA expression levels have been described (Venero *et al.*, 1999, 2001). Thus, it is essential to compare similar regions in diseased and normal control brain, before inferring a 'pathological change' in AQP4 distribution and expression level. Upregulated AQP4 was reported in astrocytes located at the periphery of MS plaques, but the plaque centre and unaffected normal appearing white matter areas were essentially devoid of AQP4 (Aoki *et al.*, 2005; Misu *et al.*, 2006). However, the stage of demyelinating activity within the MS lesions was not specified, precluding determination of any association of lesional stage with AQP4 expression.

The distribution of AQP4 at glial–fluid interfaces in the mouse spinal cord coincides with sites to which NMO-IgG binds, and is similar to the deposition pattern of Ig and complement activation products observed in actively demyelinating NMO lesions (Lucchinetti *et al.*, 2002; Lennon *et al.*, 2004). These observations make a compelling but circumstantial case for AQP4-IgG being a primary effector of NMO lesions. A recent immunohistochemical study of a single NMO case reported perivascular loss of AQP4 immunoreactivity in spinal cord lesions (Misu *et al.*, 2006). The authors contrasted this observation with high AQP4 expression in a section of normal cervical spinal cord grey matter, and with an apparent increase of AQP4 expression in reactive astrocytes of MS lesions. This study, however, did not specify the number of MS cases, the number of lesions analysed, or the stage of demyelinating activity in any of the NMO or MS lesions. Furthermore, the observed loss of AQP4 in some lesions corresponded to regions of tissue necrosis and cavitation. Although the authors suggested that functional impairment of astrocytes by AQP4-specific antibody may underlie NMO lesion pathogenesis, they did not address the potential influence of other biological factors on AQP4 expression, such as demyelinating or remyelinating activity, the extent of tissue necrosis, or the degree of astrocyte loss.

The present study describes AQP4 expression in a large series of NMO cases that are well characterized clinically and pathologically (Lucchinetti *et al.*, 2002). We compare expression patterns of AQP4 immunoreactivity in NMO lesions with patterns observed in normal brain, optic nerve and spinal cord; in acute, subacute and chronic infarcts of brain, optic nerve and spinal cord; and in acute and chronic MS lesions. We observed that the pattern of AQP4 expression in normal tissues is similar to the rim and rosette pattern of Ig deposits and products of complement activation observed in NMO lesions. In contrast to a stage-dependent loss of AQP4 in MS lesions, we observed in all NMO lesions a striking loss of AQP4 regardless of the stage of demyelinating activity, extent of tissue necrosis, or CNS region involved. We further observed AQP4 loss at

Table 1 Antibodies used for immunohistochemistry

Antibody	Clone	Dilution	Antigen retrieval	Company/source
GFAP	Polyclonal	1 : 4000	NA	Dako, Denmark
AQP4	Polyclonal	1 : 250	NA	Sigma-Aldrich, USA
NF	Monoclonal	1 : 800	Steam/EDTA	Dako, Denmark
MBP	Monoclonal	1 : 150	NA	Boehringer, Mannheim; Roche, Germany
PLP	Monoclonal	1 : 1000	NA	Serotec, USA
CNPase	Monoclonal	1 : 2000	Steam/citric buffer	Sternberger, USA
MOG	Monoclonal	1 : 200	NA	Dr Sarah Piddlesden; Cardiff, UK
MAG	Monoclonal	1 : 10	Proteinase K	Chemicon, USA
KiMIP	Monoclonal	1 : 1000	Steam	Dr Radzun; Goettingen, Germany
CD3	Monoclonal	1 : 400	Steam/citric buffer	Serotec, USA
CD8	Monoclonal	1 : 50	Steam/citric buffer	Dako, Denmark
CD20	Monoclonal	1 : 60	Steam/EDTA	Dako, Denmark
CDI38	Monoclonal	1 : 50	Steam/EDTA	Dako, Denmark
IgG	Polyclonal	1 : 10,000	Steam/EDTA	Dako, Denmark
IgM	Polyclonal	1 : 750	Steam/EDTA	Dako, Denmark
C9neo	Polyclonal	1 : 400	Steam	Dr Paul Morgan; Cardiff, UK
C9neo	Monoclonal	1 : 200	Protease 0.03%	Dr Paul Morgan; Cardiff, UK

All monoclonal antibodies are from mouse and all polyclonals from rabbit. EDTA = ethylenediaminetetraacetic acid; NA = not applicable.

sites of vasculocentric Ig deposition and complement activation in NMO lesions that lacked demyelination, but were inflammatory. These lesions were identified in both the spinal cord and medulla at the floor of the fourth ventricle, particularly involving the area postrema, a region lacking a blood–brain barrier (BBB) and rich in osmoreceptors. The pathogenic implications of these observations are discussed.

Material and methods

Archival material

The study was performed on archival brain, optic nerve and spinal cord material from nine patients with NMO, 13 with MS, nine with infarcts and five neurologically normal patients without CNS histopathological abnormalities. The study was approved by the Mayo Clinic Institutional Review Board (2067–99). Causes of death in the control cases were acute myocardial infarct (3), pneumonia (1) and unknown (1). All materials were obtained at autopsy except for two acute MS cases that were obtained surgically (diagnostic brain biopsy). Detailed clinical histories were available for all cases. The NMO cohort comprised eight women and one man, with an average age of 50 years (range 16–80 years). The clinical course was relapsing in eight patients, and monophasic in a single case. Mean disease duration was 2.4 years (SEM ± 0.8 years). All patients died from respiratory compromise directly attributable to attacks of NMO. The presenting syndrome was optic neuritis in four patients, and myelitis in five patients, with a mean interval of 19 months (range 4–41 months) between optic neuropathy and myelopathy. The MS cohort comprised: (i) 11 acute MS cases (nine women and two men) with an average age of 43 years (range 26–70 years). Mean disease duration was 4.1 months (SEM ± 13.6 months). Death was attributable to an acute MS attack associated with herniation in five cases, sepsis due to pneumonia in three and unknown in one. Two patients are still living. (ii) Two chronic cases, both women (aged 36 and 71 years) who had a secondary progressive course and mean disease duration of 18 years (6 and 30 years). Both patients died of respiratory compromise associated with pneumonia.

Neuropathological evaluation and immunohistochemistry

Specimens were fixed in 10–15% formalin and embedded in paraffin. Sections were stained with haematoxylin and eosin (HE), Luxol-fast blue-periodic acid-Schiff (LFB/PAS) and Bielschowsky silver impregnation. Immunohistochemistry was performed without modification using an avidin–biotin or an alkaline-phosphatase/anti-alkaline phosphatise (APAAP) technique as described previously (Vass *et al.*, 1986). The primary antibodies were specific for myelin proteins (myelin basic protein [MBP; Boehringer Mannheim, Germany], proteolipid protein [PLP, polyclonal; Serotec, Oxford, USA], myelin oligodendrocyte protein [MOG; Dr S Piddlesden, Department of Biochemistry, Cardiff, UK], 2′3′-cyclic-nucleotide 3′-phosphodiesterase, [CNPase; Sternberger, USA], myelin associated glycoprotein [MAG; Serotec]), glial fibrillary acidic protein (GFAP; Dako), neurofilament protein (NF; Dako), T lymphocytes (all T cells; CD3 and cytotoxic CD8 T cells; [Dako]), B lymphocytes (CD20; Dako), plasma cells (CD138; Dako), macrophages/microglial cells (KiM1P; Dr Radzun, University of Göttingen, Germany), activated complement antigen (C9neo; Dr Paul Morgan, Department of Biochemistry, Cardiff, UK), immunoglobulin G (IgG; Dako), immunoglobulin M (IgM; Dako) and AQP4 (C-terminal residues 249–323, affinity purified rabbit IgG; Sigma-Aldrich). Table 1 lists the antibodies and specific conditions used for immunohistochemistry. The primary antibodies were omitted in controls. All antibodies were incubated at 4°C overnight.

Staging of demyelinating activity in NMO and MS lesions

Lesions were classified with respect to demyelinating activity, as previously described (Bruck *et al.*, 1995). ‘Early active

demyelinating lesions' were diffusely infiltrated by macrophages containing immunoreactive products for all myelin proteins. 'Late active demyelinating lesions' were more advanced with respect to myelin degradation, and were immunoreactive for major myelin proteins (MBP and PLP), but not for MOG or CNPase. 'Remyelinating lesions' were characterized by uniformly thin and irregularly arranged myelin sheaths. 'Inactive demyelinated lesions' were completely demyelinated without evidence of active demyelination. We examined 77 lesions from 9 autopsy cases of clinically confirmed NMO. Demyelinating activity in the NMO lesions was classified immunohistochemically as 'early active' in 22, 'late active' in 18, 'inactive' in 37 and 'remyelinating' in 0. Demyelinating activity in 57 lesions from the 11 acute MS cases was classified as 'early active' in 45, 'early remyelinating' in 6 and 'inactive' in 6. The 2 chronic MS cases had no 'active' lesion, 24 'inactive', and 3 'late remyelinated' lesions (i.e. shadow plaques). Early active MS lesions in the acute MS cohort were further classified immunopathologically based on previously published criteria (Lucchinetti *et al.*, 2000), into patterns I (T cell/macrophage associated) ($n = 2$ lesions from two MS biopsy cases), II (antibody/complement associated) ($n = 30$ lesions from six cases), III (distal oligodendrogliopathy) ($n = 11$ lesions from two cases) or IV (primary oligodendrogliopathy) ($n = 2$ lesions from one case). We also evaluated AQP4 expression in nine NMO lesions and seven MS lesions with cavitation.

Results

Table 2 summarizes AQP4 immunoreactivity patterns in infarct, MS and NMO tissues relative to baseline expression in normal CNS control tissues. Specific characteristics of AQP4 immunoreactivity are discussed subsequently.

Table 2 Aquaporin-4 immunoreactivity in infarct, MS and NMO relative to baseline expression in normal controls

Normal controls	$n = 5$	GM	WM
Cerebrum		+++	+/−
Brainstem		+++	++
Spinal cord		+	++
Optic nerve		NA	++
Neurological disorders	$n = 31$	Peri lesion	Lesion
Infarct	$n = 9$		
Acute ($n = 3$)		↑↑↑	0
Subacute ($n = 3$)		↑↑↑	0
Chronic ($n = 3$)		↔	0
Chronic multiple sclerosis	$n = 2$		
Inactive ($n = 24$)		↔	0
Late remyelinating ($n = 3$)		↑↑	↑↑
Acute multiple sclerosis*	$n = 11$		
Active ($n = 45$)		↑↑↑	↑
Inactive ($n = 6$)		↑	0
Early remyelination ($n = 6$)		↑↑	↑↑
Cavitary ($n = 7$)		↑↑	0
Neuromyelitis optica†	$n = 9$		
Active ($n = 40$)		↔	0
Inactive ($n = 37$)		↔	0
Cavitary ($n = 9$)		↔	0

N = number of cases; *n*, number of lesion areas; GM = grey matter; WM = white matter; NA = not applicable; +/−, +, ++, +++ = intensity scale of AQP4 immunoreactivity in CNS control tissue; ↑, ↑↑, ↑↑↑ = degree of increase in AQP4 immunoreactivity relative to baseline expression in regionally matched CNS control tissue; ↔ = no change in AQP4 immunoreactivity relative to baseline expression in regionally matched CNS control tissue; 0 = complete loss of AQP4 immunoreactivity. *There is no difference in AQP4 immunoreactivity pattern between immunopathologically classified acute MS cases (patterns I = 2, II = 6, III = 2, IV = 1). †AQP4 immunoreactivity is also absent in inflammatory NMO foci lacking demyelination associated with vasculocentric immune complex deposition.

AQP4 immunoreactivity in normal CNS tissues

AQP4 immunoreactivity in normal tissues, at all levels of the CNS, was most intense at the glia limitans externa and the subependyma (Fig. 1A–C). Within the cerebral cortex, AQP4 immunoreactivity was concentrated in astrocytic foot processes extending to the abluminal surface of blood vessels (Fig. 1D). As is typical of astrocytes, GFAP immunoreactivity was concentrated in the cell body and soma, and did not extend to the astrocytic endfeet associated with either small or medium-sized blood vessels (Simard et al., 2003), (Fig. 1E). Cerebral white matter showed limited AQP4 immunoreactivity, which was restricted to the abluminal surface of occasional penetrating blood vessels (Fig. 1F). Within the brainstem (midbrain to caudal medulla), AQP4 immunoreactivity was most intense in subependymal regions at the floor of the fourth ventricle (Fig. 1G). Brainstem white matter exhibited a mesh-like pattern of AQP4 immunoreactivity, with prominent perivascular staining in a rim and rosette pattern. In the spinal cord, AQP4 immunoreactivity was prominent within both grey and white matter (Fig. 1H). AQP4 immunoreactivity in the optic nerve exhibited meshwork and rim and rosette vasculocentric patterns (Fig. 1I), similar to those seen in brainstem and spinal cord white matter.

AQP4 immunoreactivity in other neurological disorders

The intensity and distribution of AQP4 immunoreactivity in brain, optic nerve and spinal cord infarcts were compared with the baseline expression patterns observed in regionally matched normal control tissues. In acute infarcts (<12 h; one cerebral and two spinal cord) and subacute infarcts (<7 days; one cerebral and two spinal cord), AQP4 was lost in the necrotic centre and diffusely increased at the periphery of the infarct (Fig. 2A and E). A similar pattern of GFAP immunoreactivity was seen in the necrotic centre and ischaemic periphery (Fig. 2B). Higher magnification demonstrated increased AQP4 outlining the cytoplasmic surface of reactive astrocytes (Fig. 2C), whereas GFAP was more concentrated in the cell body (Fig. 2D). AQP4 was lost in the necrotic zone (Fig. 2A, E and F). Chronic infarcts (>2 years; two cerebral

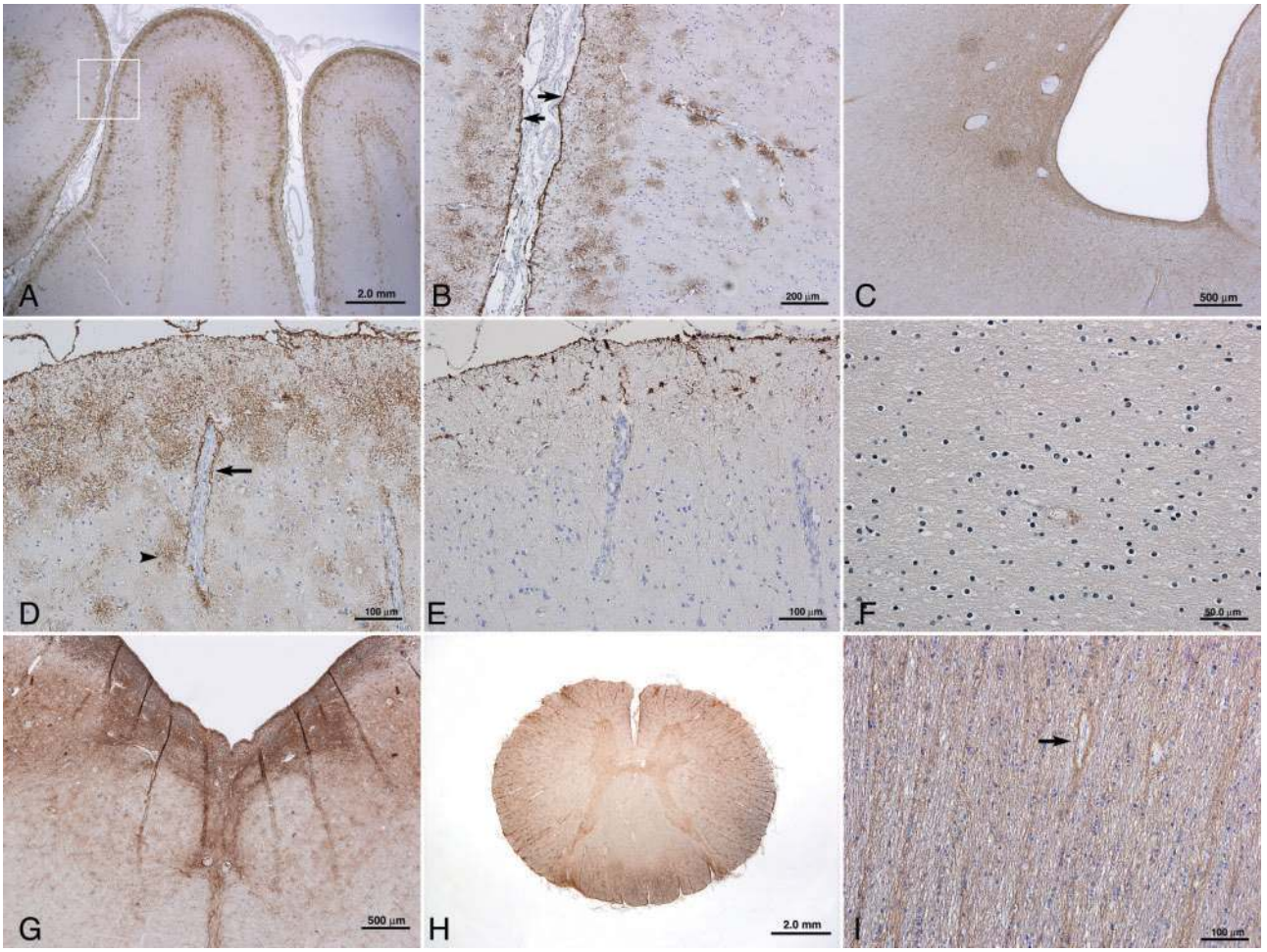

Fig. 1 AQP4 immunoreactivity (IR) in normal CNS tissues. (**A**) AQP4 is concentrated at the glia limitans externa, throughout the cerebral cortex and at the grey–white junction. (**B**) Higher magnification of boxed region in A demonstrates intense AQP4 at the glia limitans (arrows) and a rosette pattern of staining in the underlying cortex. (**C**) AQP4 is concentrated in the subependymal region. (**D**) AQP4 is intense at the abluminal surface of penetrating cortical blood vessels in a rim pattern (arrow) and at astrocytic foot processes abutting vessels in a rosette pattern (arrowhead). (**E**) GFAP is concentrated at the glia limitans and astrocyte cell body, but does not label astrocytic endfeet associated with small to medium sized vessels. (**F**) AQP4 is minimal in normal cerebral white matter, apart from occasional penetrating capillaries. (**G**) AQP4 is intense at the floor of the fourth ventricle. (**H**) Spinal cord white and grey matter show moderate diffuse AQP4. (**I**) Optic nerve shows diffuse mesh-like and vasculocentric (arrow) AQP4 IR. **A**–**D**, **F**–**I**, AQP4 Immunohistochemistry (IHC); **E**, GFAP IHC.

and one optic nerve) demonstrated no increase in AQP4 immunoreactivity at the periphery, while cavitary regions were devoid of AQP4.

AQP4 immunoreactivity in MS lesions is stage-dependent

AQP4 expression in MS lesions correlated with the stage of demyelinating activity. In acute MS cases immunopathologically classified as patterns I, II, III or IV, the pattern of AQP4 immunoreactivity was identical. AQP4 was diffusely increased in the periplaque white matter of early (Fig. 3A) and late active lesions, and outlined the cytoplasmic surface of enlarged reactive astrocytes dispersed throughout the active lesion centre (Fig. 3B). Early remyelinating lesions demonstrated a diffuse increase in AQP4 immunoreactivity in both the periplaque white matter and lesion centre (Fig. 3C), and also outlined the cytoplasmic surface of reactive astrocytes (Fig. 3D). In contrast, inactive lesions identified within the acute MS cohort were devoid of AQP4 (Fig. 3E), despite the continued presence in some lesions of PAS-positive macrophages that lacked myelin degradation products. In both chronic MS cases, AQP4 was absent in inactive long-standing plaques (Fig. 3F), but was diffusely increased within late remyelinated shadow plaques. AQP4 was absent in all seven cavitary acute MS lesions.

In active pattern II MS lesions (Fig. 4A), Ig and complement deposits were distributed in a pattern quite distinct from the striking perivascular rosette and rim pattern of Ig and complement activation product deposition described in NMO lesions (Lucchinetti *et al.*, 2002).

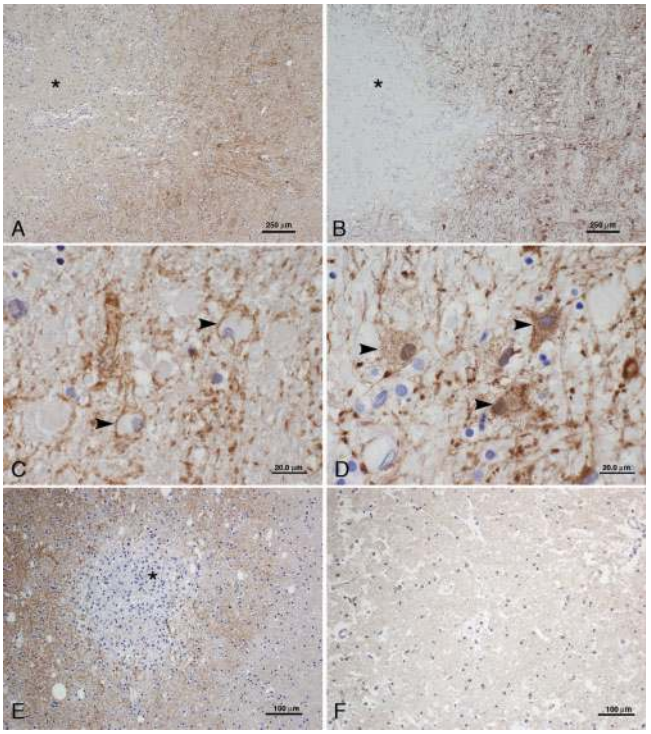

Fig. 2 AQP4 immunoreactivity (IR) in early acute (**A**–**D**) and subacute (**E**–**F**) infarcts. (**A**) The early acute infarct demonstrates loss of AQP4 in the necrotic centre (*), with increased IR in the periphery. (**B**) With GFAP, there is a similar pattern and distribution of IR, absent in the necrotic centre (*), and increased at the periphery. (**C**) Higher magnification of the infarct periphery in **A** demonstrates increased AQP4 outlining the cytoplasmic surface of reactive astrocytes (arrowheads). (**D**) Higher magnification of the infarct periphery in **B** demonstrates GFAP is similarly increased in reactive astrocytes, but concentrated in cell bodies (arrowheads). (**E**) The subacute infarct also demonstrates increased AQP4 IR in the periphery, with relative lack of AQP4 IR in macrophage-rich necrotic areas (*). (**F**) There is absence of AQP4 in the necrotic zone. **A**, **C**, **E**, **F**, AQP4 IHC; **B**, **D**, GFAP IHC.

The inflammatory infiltrates in pattern II MS lesions were lymphocytic and products of complement activation were less pronounced in degree, and were detected on degenerating myelin sheaths, within macrophages and on oligodendrocytes along the active plaque edge (Fig. 4B) (Lucchinetti *et al.*, 2000). AQP4 immunoreactivity was less intense in the plaque centre relative to its increased expression in the periplaque white matter, and outlined the cytoplasm of reactive astrocytes, as well as astrocytic foot processes surrounding blood vessels (Fig. 4C).

AQP4 immunoreactivity in NMO lesions

The pattern of AQP4 expression in NMO lesions was fundamentally different. No AQP4 immunoreactivity was detectable in any lesion, irrespective of stage of demyelinating activity. Actively demyelinated NMO lesions (Fig. 4D) contained granulocytes and eosinophils, and exhibited a striking vasculocentric deposition of Ig and the C9neo product of complement activation (Fig. 4E) in a rim and rosette pattern (Fig. 4E, inset), in regions of AQP4 loss (Fig. 4F). Periplaque white matter demonstrated a similar degree of AQP4 immunoreactivity as normal regionally matched control tissue (Fig. 4F). The identical pattern of AQP4 loss independent of demyelinating stage was also observed in the optic nerve of a single NMO case [early active (Fig. 5A and B), inactive, and cavitary lesion areas], in contrast to the stage-dependent pattern of periplaque and lesion AQP4 expression observed in early active (Fig. 5C, D), remyelinated, inactive and cavitary optic nerve lesion areas from a single acute MS case.

An unanticipated observation was loss of AQP4 in spinal cord (Fig. 6C) and brainstem regions characterized by eosinophil and plasma cell infiltrates and vasculocentric deposits of IgM, IgG (Fig. 6A) and complement activation products (Fig. 6B), but lacking evidence of demyelination ($n = 5$ cases) (Fig. 6D and E). These regions appeared rarefied, particularly around blood vessels (Fig. 6D), and despite AQP4 loss, they retained normal staining of all myelin proteins [MBP, PLP, CNPase, MAG, MOG (Fig. 6E)], and lacked macrophages containing myelin degradation products. Axons were structurally preserved with no evidence of acute axonal pathology (Fig. 6F).

Of particular note, three of the NMO cases had inflammatory foci lacking demyelination associated with AQP4 loss situated below the floor of the fourth ventricle extending laterally along the subependymal surface (Fig. 7). The involved tissue appeared rarefied (Fig. 7A), and contained numerous perivascular and parenchymal CD138+ plasma cells (Fig. 7B) and eosinophils (Fig. 7C). Myelin was preserved in the subependymal white matter (Fig. 7D). IgG and IgM deposits were diffuse (Fig. 7E), as well as vasculocentric (Fig. 7G), and serial sections revealed they co-localized with products of complement activation (Fig. 7H) and regions of AQP4 loss (Fig. 7F and I). These inflammatory foci associated with AQP4 loss extended into the adjacent area postrema (Fig. 7G–I), a site known to lack a BBB.

Despite a complete loss of AQP4 immunoreactivity (Fig. 8A and C), reactive GFAP positive astrocytes were dispersed throughout these inflammatory, non-demyelinated NMO foci (Fig. 8B and D). This is in contrast to active (Fig. 8E and F; Fig. 3B) and remyelinating (Fig. 3C and D) MS lesions, as well as acute and subacute infarcts (Fig. 2A, C and E), in which AQP4 immunoreactivity is diffusely increased, and outlines the cytoplasmic surface of GFAP positive astrocytes.

Discussion

The relationship between MS and NMO has long been debated. We previously reported a unique pattern of tissue destruction in active NMO lesions characterized by

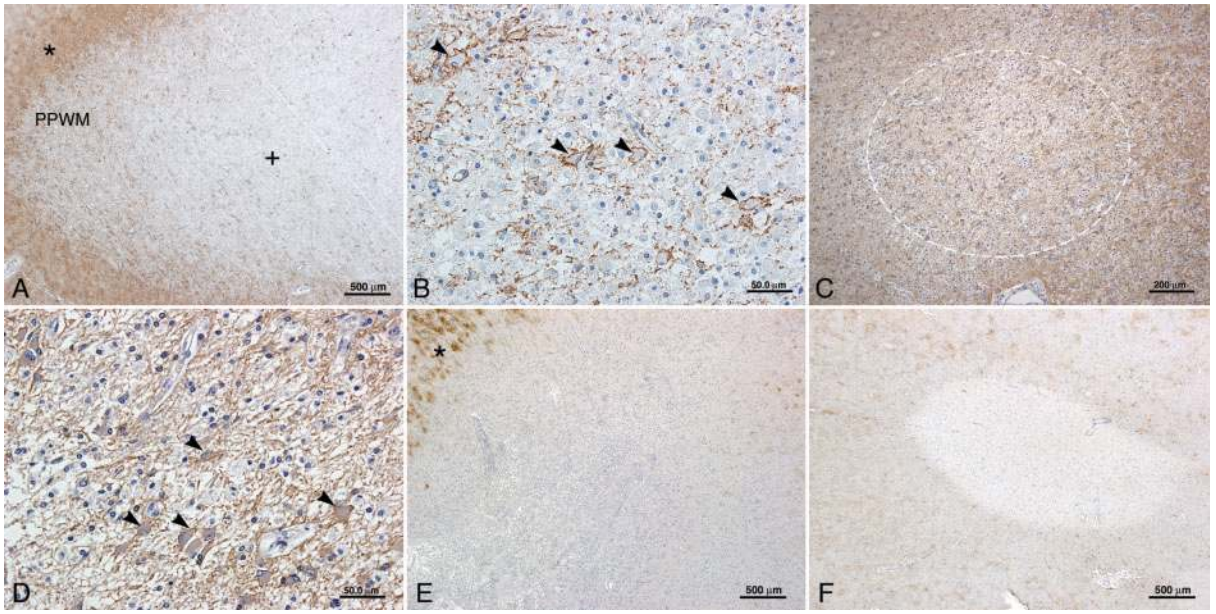

Fig. 3 Stage-dependent pattern of AQP4 immunoreactivity (IR) in active (**A, B**), early remyelinated (**C, D**) and inactive (**E, F**) MS lesions. (**A**) An active MS lesion demonstrates increased AQP4 IR that is marked in the adjacent cortical grey matter (*) and periplaque white matter (PPWM), and moderate in the lesion centre (+). (**B**) Higher magnification of the active lesion centre demonstrates AQP4 outlining the cytoplasmic surface of reactive astrocytes (arrowheads) and their processes. (**C**) An early remyelinated MS lesion (circle) shows diffuse increase in AQP4 extending throughout the lesion, and surrounding PPWM. (**D**) AQP4 stains the cytoplasmic surface of reactive astrocytes (arrowheads) in an early remyelinated lesion. (**E**–**F**). Inactive MS lesions from an acute case (**E**) and a chronic case (**F**) show complete loss of AQP4; (*) indicates normal grey matter AQP4 IR. **A**–**F**, AQP4 IHC.

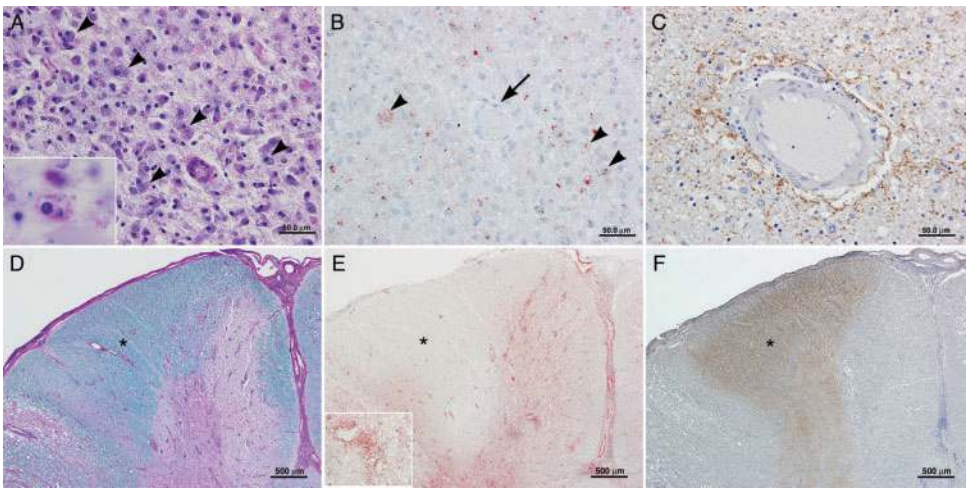

Fig. 4 AQP4 immunoreactivity (IR) in acute pattern II MS (**A**–**C**) and NMO (**D**–**F**) lesions. (**A**) Numerous macrophages containing myelin debris are dispersed throughout the active lesion (arrowheads and inset; LFB/PAS). (**B**) C9neo antigen is present within macrophages (arrowheads), but absent around blood vessels (arrow). (**C**) Higher magnification reveals AQP4 IR is prominent in a rosette pattern surrounding a penetrating blood vessel in the lesion. (**D**) In NMO, there is extensive demyelination involving both grey and white matter (LFB/PAS); *indicates preserved myelin in the PPWM. (**E**) C9neo is deposited in a vasculocentric rim and rosette pattern (inset) within the active lesions, but not in the PPWM. (**F**) The lesions lack AQP4, which is retained in the PPWM (*) and grey matter. **A**, **D**, LFB/PAS; **B**, **E**, C9neo IHC; **C**, **F**, AQP4 IHC.

eosinophil and neutrophil infiltration, vascular fibrosis and intense vasculocentric deposition of Ig and products of complement activation in a characteristic 'rim' and 'rosette' pattern (Lucchinetti *et al.*, 2002). Based on those findings, we suggested that humoral autoimmunity targeting an antigen in the perivascular space may play a role in the pathogenesis of NMO. Lennon *et al.* subsequently identified a specific marker autoantibody (NMO-IgG), which interacts selectively with the AQP4 water channel (Lennon *et al.*, 2005). AQP4 is concentrated at the astrocytic endfeet, which are typically GFAP-negative (Frigeri *et al.*, 1995; Bushong *et al.*, 2002; Simard *et al.*, 2003). Whereas GFAP-positive processes do not systematically cover smaller vessels (<16 μm) and capillaries, AQP4 expression outlines

the entire network of vessels (Simard *et al.*, 2003; Lennon *et al.*, 2005). A pathogenic role for NMO-IgG remains to be proven, but the strategic location of AQP4 at the BBB strengthens our original hypothesis of a perivascular target antigen.

The present study describes a unique pattern of AQP4 loss in nine of nine NMO cases. This pattern is unrelated to stage of demyelinating activity and is distinct from the patterns of AQP4 expression observed in MS, infarcts and normal controls. Changes in the intensity of AQP4 immunoreactivity in MS lesions were dependent on the stage of demyelination. The increase in AQP4 immunoreactivity observed in the periplaque white matter and within reactive astrocytes of active MS lesions is consistent with published studies (Aoki *et al.*, 2005; Misu *et al.*, 2006). However, we also observed complete loss of AQP4 immunoreactivity in inactive MS lesions sampled from both the acute and chronic phases of the disease. This contradicts the findings of Misu *et al.* (2006) whose study concluded that AQP4 is not lost in MS lesions, but in which the stage of demyelinating activity was not reported.

It is not unexpected to find AQP4 expression increased in actively demyelinating and remyelinating MS lesions, since astrocytic proliferation is a physiological host response to inflammation. Similarly, it is not unexpected for AQP4 expression to be reduced or undetectable in inactive gliotic and quiescent non-inflammatory MS lesions. Increased AQP4 immunoreactivity outlining GFAP positive reactive astrocytes and their processes was observed in the periplaque and lesion centre of active and remyelinating MS lesions, and in the periphery of infarcts. However, both active MS and NMO lesions are characterized by a proliferative astrocytic response, yet AQP4 immunoreactivity was not observed in either the periplaque or lesion centre of any NMO lesion, regardless of location, or stage of demyelinating activity. These findings suggest a targeted attack against AQP4. The presence of GFAP positive

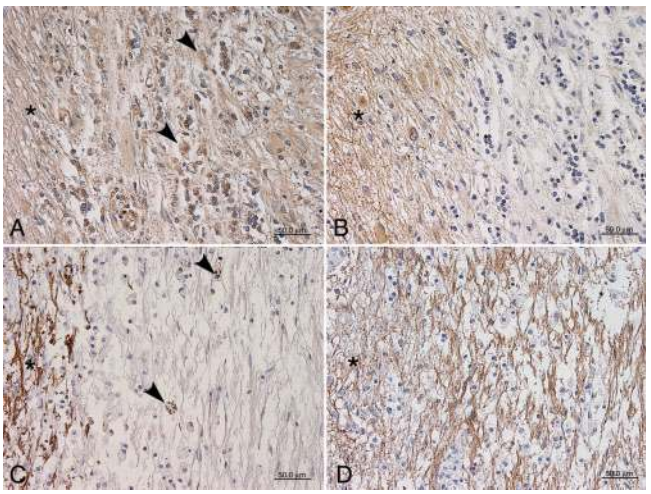

Fig. 5 Comparison of AQP4 immunoreactivity (IR) in active NMO (**A, B**) and MS (**C, D**) optic nerve lesions. (**A**) Active demyelination with macrophages containing MOG-immunoreactive myelin debris (arrowheads), adjacent to PPWM (*). (**B**) AQP4 is lost in the active lesion, but retained in the PPWM (*). (**C**) Active demyelination with macrophages containing PLP-immunoreactive myelin debris (arrowheads), adjacent to PPWM (*). (**D**) AQP4 IR is increased in both the active lesion and PPWM (*). **A**, MOG IHC; **B, D**, AQP4 IHC; **C**, PLP IHC.

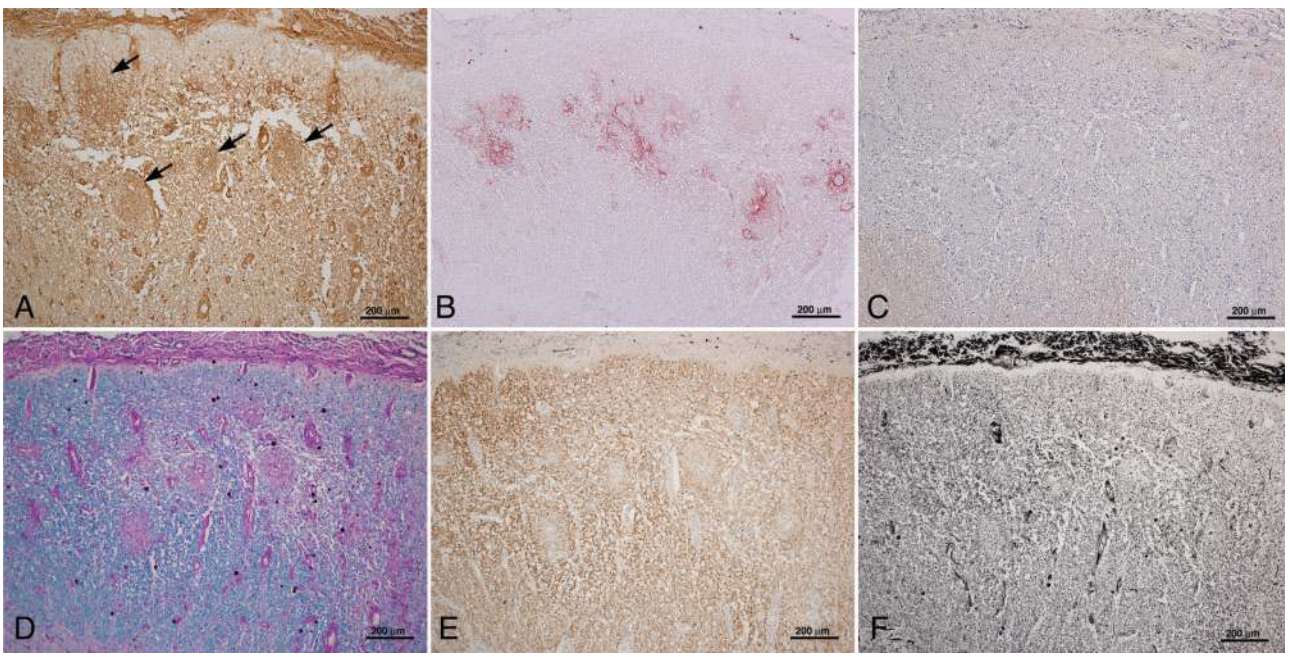

Fig. 6 Spinal cord AQP4 loss in inflammatory NMO foci lacking demyelination. (**A**–**B**) Immune complexes (IgG, **A**; C9neo, **B**) are deposited in a rosette pattern surrounding thickened, hyalinized vessels (arrows). (**C**–**F**) The lesion is characterized by complete loss of AQP4 IR (**C**; note residual AQP4 in grey matter at lower left), with preservation of myelin (**D**, LFB/PAS; **E**, MOG) and axons (**F**, Bielschowsky).

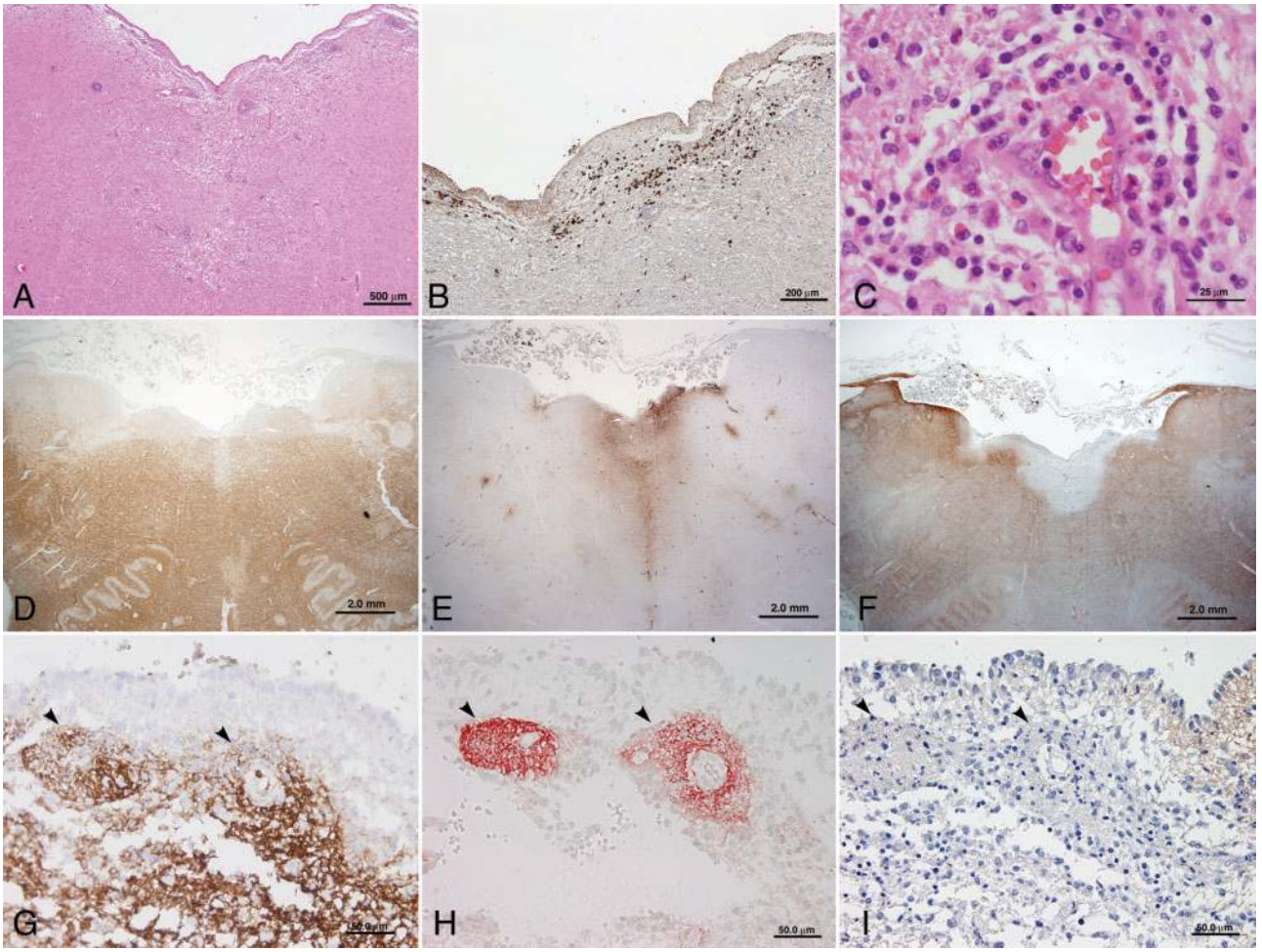

Fig. 7 Medullary floor of the fourth ventricle AQP4 loss in inflammatory NMO foci lacking demyelination. (**A**–**C**) Patchy perivascular inflammatory infiltrate and parenchymal rarefaction are noted at low power (**A**, **H** & **E**). Major components of the inflammatory infiltrates include plasma cells (**B**, CD138), and eosinophils (**C**, **H** & **E**), but macrophages are scarce. (**D**–**F**) There is myelin preservation (**D**, MOG), while IgM is prominent in subventricular zones. (**E**, IgM). Note that AQP4 loss is most profound in region of IgM deposition (**F**, AQP4). (**G**–**I**) In the area postrema: subependymal vessels (arrowheads) show a rosette pattern of staining for IgM (**G**), C9neo (**H**) and loss of AQP4 (**I**).

reactive astrocytes within inflammatory non-demyelinated NMO lesions, despite the complete absence of AQP4 immunoreactivity, argues against AQP4 loss in NMO lesions being secondary to astrocyte loss. Our finding of stage-dependent differences in AQP4 expression in MS lesions, in contrast to the absence of AQP4 in all NMO lesions regardless of demyelinating stage, suggests that different pathogenic mechanisms underlie disease initiation and evolution in these two disorders.

This study also provides a plausible explanation for the rim and rosette pattern of Ig and complement activation product deposits that we reported previously as a distinctive characteristic of NMO lesions (Lucchinetti *et al.*, 2002). The finding of an identical staining pattern of AQP4 in normal brain, optic nerve and spinal cord localizing to astrocytic endfeet in the perivascular glia limitans, suggests that the rim and rosette pattern of Ig and terminal complement deposition reflects the regional density of AQP4 molecules (Nielsen *et al.*, 1997; Venero *et al.*, 1999). The report of Misu *et al.* (2006) emphasized increased AQP4 immunoreactivity within normal central spinal cord grey matter. We additionally noted prominent staining of white matter within normal optic nerve, brainstem and spinal cord tissues, in contrast to limited expression of AQP4 in supratentorial white matter. The widespread expression of AQP4 in the brain is paradoxical in face of the typically optic–spinal predominant locations of NMO lesions and predilection for brainstem. Regional differences in AQP4 concentration could contribute to this paradox, as well as regional differences in the spatial distribution or molecular orientation of AQP4 epitopes on astrocytic endfeet that might preclude efficient complement activation or intermolecular cross-linking at some sites (Lennon, 1978; Lennon *et al.*, 1984, 2005).

Given the inherently destructive nature of NMO pathology, it is important to determine whether AQP4 loss in NMO is truly disease-specific, or rather reflects tissue injury or loss of cellular elements and antigen

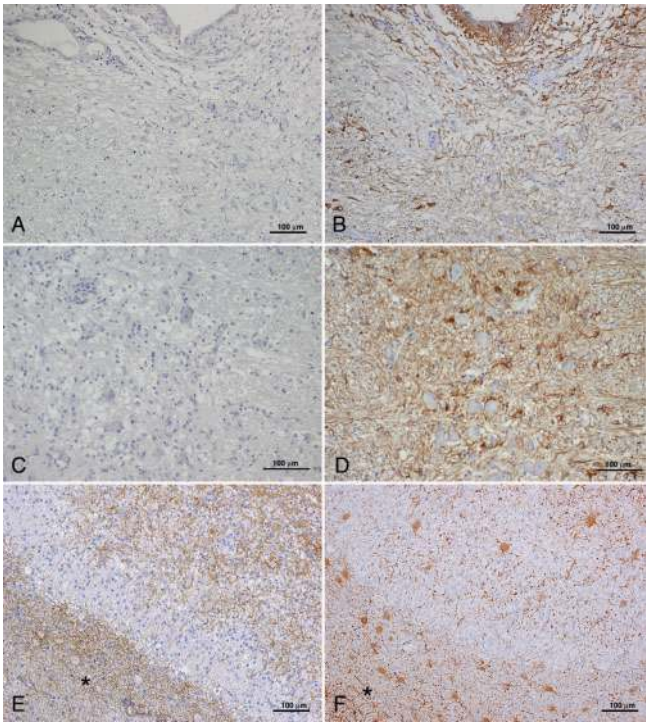

Fig. 8 AQP4 and astrocytes in NMO and MS. (**A**–**D**) There is loss of AQP4 in the medullary subependyma (**A**) and raphe (**C**), despite astrogliosis associated with the presence of GFAP immunoreactive astrocytes (**B**, **D**). (**E**–**F**) Early MS lesion shows increased AQP4 (**E**) in the PPWM (*), the expanding macrophage rich border and lesion centre. With GFAP (**F**), a similar increased distribution associated with multiple reactive astrocytes is noted. *PPWM. **A, C, E**, AQP4 IHC; **B**, **D**, **F**, GFAP IHC.

degradation associated with necrosis. Therefore, we examined AQP4 immunoreactivity in non-necrotic and necrotic regions sampled from acute, subacute and chronic infarcts. Our observations of enhanced AQP4 immunoreactivity in the periphery of acute and subacute non-necrotic ischaemic foci are consistent with published studies (Aoki *et al.*, 2003). In a rat ischaemia model, AQP4 mRNA expression after middle cerebral artery occlusion was increased in the region surrounding infarcted cortex during the observation period (1–7 days, maximal at day 3), and the change was related to the generation and resolution of brain oedema. The increase of AQP4 immunoreactivity in the periphery of acute and subacute infarcts may therefore reflect the participation of AQP4 in the development of oedema. In contrast, all necrotic ischaemic lesions lacked AQP4 immunoreactivity, regardless of infarct stage. AQP4 loss was also observed in cavitated demyelinated regions analysed from both NMO and acute fulminant MS lesions. Loss of AQP4 immunoreactivity in these circumstances is not surprising, because astrocytes are destroyed during necrosis, regardless of the initiating disease. It is, therefore, critical to evaluate non-necrotic NMO lesions in order to confirm disease-specific associations.

Our findings in spinal and brainstem NMO lesions of AQP4 loss in foci that were inflammatory but neither demyelinated nor necrotic, and co-localizing with intense vasculocentric deposition of immune complexes, strongly implicate a complement-activating AQP4-specific autoantibody as the initiator of the NMO lesion. Small amounts of circulating IgG normally gain access to the CNS because the BBB is not absolutely impenetrable (Brimijoin *et al.*, 1990). NMO may indeed be an antibody-mediated disease. However, our findings to date have not excluded a role for effector T cells in NMO pathogenesis.

Our study revealed another novel pathological finding in NMO, namely lesions in the medullary tegmentum at the floor of the fourth ventricle involving the subependymal region and the area postrema. Recent MRI studies have established conclusively that lesions in NMO may target the brain, even relatively early in the course of the disease, and that certain brain lesions are far more common in NMO than in MS (Pittock *et al.*, 2006*a*,*b*). In 10% of the cases, NMO brain lesions affect the hypothalamus and brainstem, especially the periventricular and subependymal regions. Clinical reports have described endocrine dysfunction in NMO (Vernant *et al.*, 1997), as well as intractable hiccups and nausea in 8 out of 47 cases of relapsing NMO (Misu *et al.*, 2005). In six of the latter report's cases, MRI revealed medullary lesions involving the ventricular and spinal canal regions, the nucleus tractus solitarius and the area postrema. Our observations likely reflect the pathological substrate underlying these clinical and imaging correlates of NMO.

The area postrema, like other circumventricular organs, shows intense AQP4 expression and has characteristic 'hypendymal' features, namely a neurovascular plexus with a loose glial bed, a thin ependymal cover and lack of BBB (Goren *et al.*, 2006). Expression of AQP4 in astrocytic endfeet and the glia limitans is critical for normal regulation of water fluxes at the blood–brain and CSF–brain interfaces. Neurons and astrocytes of the area postrema are an important target for circulating signals regulating blood pressure, cerebral blood flow and osmolarity, including angiotensin II, arginine, vasopressin and atriopeptins (Simard and Nedergaard, 2004). This region also serves as an interface between the immune system and the brain. It contains receptors for circulating cytokines and following peripheral challenges with immunostimulants, may harbour immunocytes expressing cytokine immunoreactivity, such as IL-1β. In the area postrema, mast cells are located subependymally and in close proximity to blood vessels, suggesting that their products may regulate local blood flow and blood vessel permeability. The area postrema has robust connections with other CNS areas involved in osmoregulation and brain volume homeostasis, including the magnocellular hypothalamic nuclei, and with areas involved in immunomodulation, such as the paraventricular nucleus. Thus autoimmune targeting of this region in NMO may disrupt several homeostatic mechanisms which may result in impaired cerebral

blood flow autoregulation, cerebral oedema and immune dysregulation.

In summary, we have documented two basic pathologies in NMO, both associated with loss of AQP4 immunoreactivity. The most prevalent lesion type involved the spinal cord and optic nerves, and AQP4 loss was in the context of vasculocentric immune complex deposition, active demyelination and vascular hyperplasia with hyalinization. These lesions were often cavitary, and involved both grey and white matter in the spinal cord. The less frequent lesion type was found in the spinal cord and medulla extending into the area postrema, and was highly inflammatory. AQP4 loss was associated with vasculocentric IgG and IgM deposits and complement activation, and tissue rarefaction, but there was no evidence of demyelination. Whether these inflammatory non-demyelinated brainstem lesions progress to demyelinated cavitary NMO lesions is uncertain, but unlikely in light of recent MRI reports describing reversible T2-weighted non-enhancing signal abnormalities corresponding to the area postrema in patients who recovered from intractable hiccups and vomiting (Misu *et al.*, 2005). Furthermore, in contrast to the severe clinical manifestations of lesions involving the optic nerves and spinal cord in NMO patients, brainstem lesions in NMO are often asymptomatic, and have been observed by imaging to resolve rapidly in some patients (Pittock *et al.*, 2006*a*,*b*). It is plausible, therefore, that these medullary inflammatory non-demyelinated NMO lesions reflect a transient functional impairment of the astrocyte's capacity to mediate water flux on initial binding of IgG to AQP4 that may be rapidly compensated in regions richly endowed with AQP4. It remains to be determined whether these two NMO lesion types reflect different pathogenic mechanisms in lesion formation, or alternatively represent different anatomical region-specific responses to the same pathogenic mechanism. Proof of the pathogenicity of AQP4-specific IgG will require the induction of the characteristic vasculocentric lesions in the spinal cord and optic nerve of animals by passive transfer of AQP4-IgG or by active immunization with AQP4.

Acknowledgements

The authors thank Patricia Ziemer for her expert technical assistance and Peggy Chihak for photographic assistance. Study supported in part by MSIF Du Pre Grant (SFR), NIH RO1-NS049577-01-A2 (CFL), NMSS RG 3185-B-3 (CFL) and the Ralph C. Wilson Medical Research Foundation (VL).

References

Amiry-Moghaddam M, Ottersen OP. The molecular basis of water transport in the brain. [Review]. Nat Rev Neurosci 2003; 4: 991–1001.

Aoki K, Uchihara T, Duyckaerts C, Nakamura A, Hauw JJ, Wakayama Y. Enhanced expression of aquaporin-4 in human brain with inflammatory diseases. Acta Neuropathol (Berl) 2005; 110: 281–8.

Aoki K, Uchihara T, Tsuchiya K, Nakamura A, Ikeda K, Wakayama Y. Enhanced expression of aquaporin-4 in human brain with infarction. Acta Neuropathol (Berl) 2003; 106: 121–4.

Brimijoin S, Balm M, Hammond P, Lennon VA. Selective complexing of acetylcholinesterase in brain by intravenously administered monoclonal antibody. J Neurochem 1990; 54: 236–41.

Bruck W, Porada P, Poser S, Rieckmann P, Hanefeld F, Kretzschmar HA, et al. Monocyte/macrophage differentiation in early multiple sclerosis lesions. Ann Neurol 1995; 38: 788–96.

Bushong EA, Martone ME, Jones YZ, Ellisman MH. Protoplasmic astrocytes in CA1 stratum radiatum occupy separate anatomical domains. J Neurosci 2002; 22: 183–92.

Frigeri A, Gropper MA, Turck CW, Verkman AS. Immunolocalization of the mercurial-insensitive water channel and glycerol intrinsic protein in epithelial cell plasma membranes. Proc Natl Acad Sci USA 1995; 92: 4328–31.

Goren O, Adorjan I, Kalman M. Heterogeneous occurrence of aquaporin-4 in the ependyma and in the circumventricular organs in rat and chicken. Anat Embryol (Berl) 2006; 211: 155–72.

Jung J, Bhat R, Preston G, Guggino W, Baraban J, Agre P. Molecular characterization of an aquaporin cDNA from brain: candidate osmoreceptor and regulator of water balance. Proc Natl Acad Sci USA 1994; 91: 13052–6.

Keegan M, Pineda AA, McClelland RL, Darby CH, Rodriguez M, Weinshenker BG. Plasma exchange for severe attacks of CNS demyelination: predictors of response. Neurology 2002; 58: 143–6.

Lennon VA. Myasthenia gravis: a prototype immunopharmacological disease. In: Miescher PA, editor. The Menarini series on immunopathology. Vol. . Basel: Schwabe & Co; 1978. p. 178–98.

Lennon VA, Kryzer TJ, Pittock SJ, Verkman AS, Hinson SR. IgG marker of optic-spinal MS binds to the aquaporin-4 water channel. J Exp Med 2005; 202: 473–7.

Lennon VA, Lambert EH, Griesmann GE. Membrane array of acetylcholine receptors determines complement-dependent mononuclear phagocytosis in experimental myasthenia gravis. Fed Proc 1984; 43: 1764.

Lennon VA, Wingerchuk DM, Kryzer TJ, Pittock SJ, Lucchinetti CF, Fujihara K, et al. A serum autoantibody marker of neuromyelitis optica: Distinction from multiple sclerosis. Lancet 2004; 364: 2106–12.

Lucchinetti C, Parisi J, Bruck W. The pathology of multiple sclerosis. Neurol Clin 2005; 23: 77–105.

Lucchinetti CF, Bruck W, Parisi J, Scheithauer B, Rodriguez M, Lassmann H. Heterogeneity of multiple sclerosis lesions: implications for the pathogenesis of demyelination. Ann Neurol 2000; 47: 707–17.

Lucchinetti CF, Mandler RN, McGavern D, Bruck W, Gleich G, Ransohoff RM, et al. A role for humoral mechanisms in the pathogenesis of Devic's neuromyelitis optica. Brain 2002; 125: 1450–61.

Manley GT, Fujimura M, Ma T, Noshita N, Filiz F, Bollen AW, et al. Aquaporin-4 deletion in mice reduces brain edema after acute water intoxication and ischemic stroke. Nat Med 2000; 6: 159–63.

Misu T, Fujihara K, Nakamura M, Murakami K, Endo M, Konno H, et al. Loss of aquaporin-4 in active perivascular neuromyelitis optica: a case report. Tohoku J Exp Med 2006; 209: 269–75.

Misu T, Fujihara K, Nakashima I, Sato S, Itoyama Y. Intractable hiccup and nausea with periaqueductal lesions in neuromyelitis optica. Neurology 2005; 65: 1479–82.

Nicchia GP, Nico B, Camassa LMA, Mola MG, Loh N, Dermietzel R, et al. The role of aquaporin-4 in blood-brain barrier development and integrity: studies in animal and cell culture models. Neuroscience 2004; 129: 935–45.

Nielsen S, Nagelhus EA, Amiry-Moghaddam M, Bourque C, Agre P, Ottersen OP. Specialized membrane domains for water transport in glial cells: high resolution immunogold cytochemistry of aquaporin-4 in rat brain. J Neurosci 1997; 17: 171–80.

O'Riordan JI, Gallagher HL, Thompson AJ, Howard RS, Kingsley DP, Thompson EJ, et al. Clinical, CSF, and MRI findings in Devic's neuromyelitis optica. J Neurol Neurosurg Psychiatry 1996; 60: 382–7.

Pittock SJ, Weinshenker BG, Lucchinetti CF, Wingerchuk DM, Corboy JR, Lennon VA. Neuromyelitis optica brain lesions localized to sites of high aquaporin-4 expression. Arch Neurol 2006a; 63: 964–8.

Pittock SJ, Lennon VA, Krecke K, Wingerchuk DM, Lucchinetti CF, Weinshenker BG. Brain abnormalities in neuromyelitis optica. Arch Neurol 2006b; 63: 390–6.

Saadoun S, Papdopoulos MC, Davies DC, Krishna S, Bell BA. Aquaporin-4 expression is increased in oedematous human brain tumors. J Neurol Neurosurg Psychiatry 2002; 72: 262–5.

Simard M, Arcuino G, Takano T, Liu Q, Nedergaard M. Signaling at the gliovascular interface. J Neurosci 2003; 23: 9254–62.

Simard M, Nedergaard M. The neurobiology of glia in the context of water and ion homeostasis. Neuroscience 2004; 129: 877–96.

Taniguchi M, Yamashita T, Kumura E, Tamatani M, Kobayashi A, Yokawa T, et al. Induction of aquaporin-4 water channel mRNA after focal ischemia in rat. Brain Res Mol Brain Res 2000; 78: 131–7.

Vajda Z, Pedersen M, Fuchtbauer EM, Wertz K, Stodkilde-Jorgensen H, Sulyok E, et al. Delayed onset of brain edema and mislocalization of aquaporin-4 in dystrophin-null transgenic mice. Proc Natl Acad Sci USA 2002; 99: 13131–6.

Vass K, Lassmann H, Wekerle H, Wisniewski HM. The distribution of Ia antigen in the lesions of rat acute experimental allergic encephalomyelitis. Acta Neuropathol (Berl) 1986; 70: 149–60.

Venero JL, Vizuete ML, Ilundain AA, Machado A, Echevarra M, Cano J. Detailed localization of aquaporin-4 messenger RNA in the CNS; preferential expression in periventricular organs. Neuroscience 1999; 94: 239–50.

Venero JL, Vizuete ML, Machado A, Cano J. Aquaporins in the central nervous system. [Review]. Prog Neurobiol 2001; 63: 321–36.

Vernant JC, Cabre P, Smadja D, Merle H, Caubarrere I, Mikol J, et al. Recurrent optic neuromyelitis with endocrinopathies: a new syndrome. Neurology 1997; 48: 58–64.

Warth A, Mittlebronn M, Wolburg H. Redistribution of the water channel protein aquaporin-4 and the K+ channel protein Kir4.1 differs in low and high grade human brain tumors. Acta Neuropathol (Berl) 2005; 109: 418–26.

Wingerchuk DM, Hogancamp WF, O'Brien PC, Weinshenker BG. The clinical course of neuromyelitis optica (Devic's syndrome). Neurology 1999; 53: 1107–14.

Wingerchuk DM, Lennon VA, Pittock SJ, Lucchinetti CF, Weinshenker BG. Revised diagnostic criteria for neuromyelitis optica. Neurology 2006; 66: 1485–9.